Research in Microbiology 173 (2022) 103937

Contents lists available at ScienceDirect

Research in Microbiology

journal homepage: www.elsevier.com/locate/resmic

Original Article

Pal depletion results in hypervesiculation and affects cell morphology and outer-membrane lipid asymmetry in bordetellae

Eline F. de Jonge [a, b], Ria van Boxtel [a], Melanie D. Balhuizen [c], Henk P. Haagsman [c], Jan Tommassen [a, b, *]

[a] Section Molecular Microbiology, Department of Biology, Faculty of Science, Utrecht University, Utrecht, the Netherlands
[b] Institute of Biomembranes, Utrecht University, Utrecht, the Netherlands
[c] Section Molecular Host Defence, Division Infectious Diseases & Immunology, Department of Biomolecular Health Sciences, Faculty of Veterinary Medicine, Utrecht University, Utrecht, the Netherlands

ARTICLE INFO

Article history:
Received 26 November 2021
Accepted 21 February 2022
Available online 3 March 2022

Keywords:
Bordetella
Outer-membrane vesicles
RmpM
Tol-Pal system
Peptidoglycan-associated lipoprotein

ABSTRACT

Current vaccines against *Bordetella pertussis* do not prevent colonization and transmission of the bacteria, and vaccine-induced immunity wanes rapidly. Besides, efficacy of vaccines for *Bordetella bronchiseptica* remains unclear. Novel vaccines could be based on outer-membrane vesicles (OMVs), but vesiculation of bordetellae needs to be increased for cost-effective vaccine production. Here, we focused on increasing OMV production by reducing the anchoring of the outer membrane to the peptidoglycan layer. Inactivation of *rmpM*, *tolR*, and *pal* failed, presumably because their products are essential in bordetellae. Conditional *pal* mutants were constructed, which were hypervesiculating under Pal-depletion conditions. SDS-PAGE and Western blot analyses showed that the protein composition of OMVs produced under Pal-depletion conditions resembled that of the outer membrane but differed from that of OMVs released by the wild type. Pal depletion affected the cell morphology and appeared to increase the amounts of cell-surface-exposed phospholipids, possibly reflecting a role for the Tol-Pal system in retrograde phospholipid transport. We also identified additional lipoproteins in bordetellae with a putative peptidoglycan-anchoring domain. However, their inactivation did not influence OMV production. We conclude that the conditional *pal* mutants could be valuable for the development of OMV-based vaccines.

1. Introduction

Bordetella pertussis and *Bordetella bronchiseptica* are β-proteobacteria that cause whooping cough in humans and similar diseases in animals, respectively. Whooping cough is most severe in children younger than one year of age. The first pertussis vaccines consisted of inactivated whole cells and were introduced around the 1940s [1]. Pertussis cases significantly dropped, but vaccine-induced side effects, e.g. neurological disorders and fever, due to presence of endotoxin in the vaccines [2], were of concern [3]. In the 1980s, the first acellular vaccine was developed in Japan, and acellular vaccines are now widely used [4]. Although vaccination rates are nowadays high, pertussis cases are resurging due to, amongst others, genetic changes in circulating *B. pertussis* strains and differences in immunity induced after vaccination with whole-cell or acellular pertussis vaccines [5–7]. Whole-cell vaccines for *B. bronchiseptica* have also been developed but their efficacy has been studied poorly and remains unclear [8].

New generation vaccines could be based on outer-membrane vesicles (OMVs). OMVs are blebs that pinch off from the outer membrane (OM) and are between 20 and 200 nm in size. Their small size allows them to be taken up easily by antigen-presenting cells [9]. Subcutaneous immunization of mice with OMVs from *B. pertussis* induced a mixed T helper (Th)1/Th2/Th17 response [10]. Efficient bacterial clearance of the nasal cavity was achieved after intranasal immunization [11]. Although OMVs are naturally released by all Gram-negative bacteria, OMV production by *Bordetella* spp. is relatively low and needs to be increased for potential vaccine development [12,13].

* Corresponding author. Section Molecular Microbiology, Department of Biology, Faculty of Science, Utrecht University, Padualaan 8, 3584 CH Utrecht, the Netherlands.
E-mail address: j.p.m.tommassen@uu.nl (J. Tommassen).

https://doi.org/10.1016/j.resmic.2022.103937

Gram-negative bacteria have an asymmetric OM, which is composed of phospholipids and lipopolysaccharides (LPS) in the inner and outer leaflet of the bilayer, respectively [14]. The OM is attached to the underlying peptidoglycan (PG) layer by covalent and non-covalent interactions. In *Escherichia coli*, Braun's lipoprotein (Lpp), the most abundant protein in this bacterium [15], covalently links the OM to the PG layer via a peptide bond between the C-terminal lysine of Lpp and *meso*-2,6-diaminopimelic acid in the PG layer [16–18]. Loss of Lpp results in hyperblebbing due to destabilization of the bacterial cell envelope [19]. Non-covalent interactions between the PG layer and the OM are mediated by e.g. OmpA in *E. coli* [20,21]. OmpA is embedded in the OM via its N-terminal β-barrel domain [22] and is able to bind the PG layer via its C-terminal domain [23]. Deletion of OmpA results in hypervesiculation in *E. coli* [24]. The homologue of OmpA in *Neisseria meningitidis* is RmpM [25,26], which stands for reduction-modifiable protein M, since its electrophoretic mobility changes in the presence of a reducing agent [27]. In contrast to OmpA, the N-terminal domain of RmpM is too short to form a β-barrel, but this domain interacts with the OM via the porins PorA and PorB [28]. The C-terminal domain of RmpM is an OmpA_C-like domain that, like the corresponding domain of OmpA, forms non-covalent interactions with the PG layer [25]. OMV production was increased in the absence of RmpM in *N. meningitidis* [29].

Also PG-associated lipoprotein (Pal) is non-covalently linked to the PG layer via a C-terminal OmpA_C-like domain [21]. Pal is anchored to the OM via its N-terminal lipid moiety [30]. Besides its role in anchoring the OM to the PG layer, Pal takes part in the Tol-Pal system, which is important for OM invagination during cell division [31]. The Tol-Pal systems consists of five proteins, namely inner-membrane (IM) proteins TolA, TolQ, and TolR, periplasmic protein TolB, and OM lipoprotein Pal [32]. Pal not only interacts with the PG layer, but it can alternatively interact with TolB [33]. The Pal–TolB complex is then recruited to the division site by TolA, where Pal is released and accumulates at the septum to stabilize the interaction between the OM and the PG layer [30]. Mutations in the *tol-pal* genes have been studied in *Salmonella enterica* serovar Typhimurium (*S.* Typhimurium), *E. coli*, and *Helicobacter pylori*, amongst others, and mutant strains showed compromised OM integrity and increased OMV production [31,32,34–36].

In bordetellae, no homologue of Lpp is present. A homologue of RmpM was found (encoded by the genes with locus tags BP0943 and BB3474 in the genome sequences of reference strains *B. pertussis* Tohama I and *B. bronchiseptica* RB50, respectively), and we have previously shown that this protein is abundant in purified OM preparations but barely present in OMVs released by *B. pertussis* [13]. Therefore, we hypothesized that RmpM is involved in anchoring the OM to the PG layer and prevents the release of OMVs. Similar to RmpM of *N. meningitidis*, the C-terminal part of *B. pertussis* RmpM contains an OmpA_C-like domain involved in PG binding, and it does not contain an N-terminal β-barrel. Therefore, RmpM might interact with the OM via porins, as described in *N. meningitidis*. Also, a Pal homologue is present in bordetellae (locus tags BP3342/BB4238), and the gene is part of a *tol-pal* operon with a similar genetic organization as in *E. coli*. Furthermore, using BLASTp searches, we have identified two additional lipoproteins (BP2019/BB1848 and BB4107) with an OmpA_C-like domain, which could, therefore, also be involved in OM-PG interaction. So far, RmpM, Pal, nor these additional lipoproteins have been functionally characterized in bordetellae. In this study, we aimed to increase OMV production by *B. pertussis* and *B. bronchiseptica* by decreasing the anchoring of the OM to the underlying PG layer. To this end, we targeted *rmpM*, *pal*, BP2019/BB1848 and BB4107 by mutagenesis, and the mutants obtained were characterized.

2. Materials and methods

2.1. Bacterial strains and growth conditions

Bacterial strains used in this study are listed in Supplementary Table S1. *E. coli* strains were cultured on lysogeny broth (LB) agar plates at 37 °C or in liquid LB while shaking at 200 rpm. *B. pertussis* and *B. bronchiseptica* strains were grown on Bordet-Gengou (BG) agar (Difco) plates supplemented with 15% (v/v) defibrinated sheep blood (bioTRADING) at 35 °C. For liquid cultures, bacteria were collected from agar plates and grown in Verwey medium [37], Stainer-Scholte (SS) medium [38], or LB while shaking at 175 rpm. To support growth of *B. pertussis*, SS medium was supplemented with 1 g/L of heptakis (2,6-di-O-methyl)-β-cyclodextrin (Sigma–Aldrich). For strain selection or plasmid maintenance, media were supplemented with ampicillin (100 μg/mL for *B. pertussis* and *E. coli* or 200 μg/mL for *B. bronchiseptica*), gentamicin (10 μg/mL), streptomycin (300 μg/mL), nalidixic acid (50 μg/mL), or cefotaxime (5 μg/mL). To induce gene expression, media were supplemented with 0.1 or 1 mM isopropyl-β-D-ʟ-thiogalactopyranoside (IPTG) for *E. coli* or *Bordetella*, respectively. Bacterial cells were inactivated for 1 h at 56 °C, unless otherwise specified.

2.2. Recombinant DNA techniques

All primers and plasmids used in this study are described in Tables S2 and S3, respectively. To overexpress *rmpM* and *pal*, the genes were amplified from *B. pertussis* strain B213 by polymerase chain reaction (PCR) using primer pairs rmpM_Fw/rmpM_Rev and pal_Fw/pal_Rev, respectively, with the Expand High Fidelity PCR system (Roche). The reverse primers contained a 3' sequence coding for a FLAG tag. The genes were cloned in pMMB67EH by substituting the *pagL* gene on $pPagL_{Bb}$ by *rmpM* or *pal*. To this end, $pPagL_{Bb}$ and the amplicons of *rmpM* or *pal* were digested with NdeI and HindIII and ligated together. *E. coli* strain DH5α was transformed with the ligation mixtures. Resulting transformants were screened by PCR, and the nucleotide sequences were verified by sequencing (Macrogen). Correct plasmids were used to transform *E. coli* strains BL21 (DE3) and SM10λ*pir* for protein overproduction in *E. coli* and transfer of the plasmids to *Bordetella*, respectively.

To construct *pal*, *tolR*, BP2019, BB1848 and BB4107 mutant strains, DNA fragments, located upstream and downstream of each target gene, were amplified using primer pairs pal_F1/pal_R1, pal_F2/pal_R2, tolR_F1/tolR_R1, tolR_F2/tolR_R2, BP2019_F1/BP2019_R1, BP2019_F2/BP2019_R2 (or BP2019_F2/BB1848_R2 to create a BB1848 knockout construct), BB4107_F1/BB4107_R1 and BB4107_F2/BB4107_R2. Amplicons were cloned into pCRII, and *E. coli* strain DH5α was transformed with the ligation mixtures. Next, the upstream and downstream fragments of each target were ligated together into one plasmid after digestion with XbaI and the restriction enzyme for which the restriction site was included in the primer (Table S2). The resulting plasmids were digested with PpuMI, Eco81I or SalI to allow for the insertion of a gentamicin-resistance cassette, which was obtained by PCR from plasmid pYRC using primer pairs Gm_Fw_P/Gm_Rev_P, Gm_Fw_E/Gm_Rev_E or Gm_Fw_S/Gm_Rev_S, respectively. Knockout constructs were then subcloned into suicide plasmid pKAS32 by SacI and XbaI restriction digestion followed by ligation. The ligation mixtures were used to transform *E. coli* strain SM10λ*pir*.

To inactivate *rmpM*, a DNA fragment, encompassing *rmpM* with upstream and downstream segments, was amplified using primers rmpM_KO_Fw and rmpM_KO_Rev. The PCR product was cloned in pCRII by XhoI and SpeI restriction digestion and ligation. The ligation mixtures were used to transform *E. coli* strain GM48 to avoid methylation of the ClaI restriction site. A gentamicin-resistance

cassette was amplified using primers Gm_Fw_C and Gm_Rev_C and inserted into the ClaI restriction site, which is present in the coding sequence of *rmpM*. The resulting *rmpM* knockout construct was cut with XbaI and SacI and ligated into XbaI–SacI-digested pKAS32.

Plasmids were transferred from *E. coli* strain SM10λ*pir* to *Bordetella* strains via conjugation. Transconjugants harboring pMMB67EH-derived plasmids were selected on agar plates containing ampicillin for plasmid selection and nalidixic acid (*B. pertussis*) or cefotaxime (*B. bronchiseptica*) for counterselection against *E. coli*. Transconjugants were screened by PCR. To create chromosomal knockouts via allelic exchange, integration of pKAS32-derived plasmids was obtained by using gentamicin for selection and the antibiotics as described above for counterselection. Transconjugants were then streaked on agar plates containing gentamicin and streptomycin to select for double crossovers. To obtain conditional mutants, the plates were supplemented with IPTG. Allelic exchange was verified by PCR.

2.3. Cell fractionation

Cells were fractionated essentially as described previously [13]. In short, *B. pertussis* was grown for two days in SS medium, and *B. bronchiseptica* was grown overnight in LB. *B. pertussis* and *B. bronchiseptica* were inactivated for 30 and 60 min, respectively, at 56 °C. Cells were harvested, washed, and converted to spheroplasts by incubation with lysozyme/EDTA. The spheroplasts were disrupted by ultrasonication, and unbroken cells were removed via low-speed centrifugation. Cell envelopes were pelleted from the supernatant by ultracentrifugation, and IM and OM were then separated via sucrose density gradient centrifugation. Sarkosyl extraction of isolated cell envelopes was preformed as described [39].

2.4. OMV isolation and quantification

OMVs were isolated as described previously [13] with some modifications. Briefly, precultures were diluted to an optical density at 600 nm (OD_{600}) of 0.05–0.1 in SS or Verwey medium and grown for 24 h in baffled flasks or glass bottles with an air:liquid ratio of 5:1 or 3.33:1, respectively. Where indicated, cultures were inactivated at 56 °C before OMV isolation. After low-speed centrifugation, the supernatants were filtered using 0.45-μm pore-size filters (Sarstedt). The filtrate was centrifuged for 2 h at 40,000 rpm and 4 °C (Beckman Coulter Optima LE-80K, Type 70 Ti rotor), and pelleted OMVs were resuspended in phosphate-buffered saline (PBS) or 2 mM Tris–HCl (pH 7.5). The quality of the OMVs was analyzed by sodium dodecyl sulfate-polyacrylamide gel electrophoresis (SDS-PAGE), and OMV yield was quantified using the Lowry DC protein assay (Bio-Rad) according to the manufacturer's instructions.

2.5. Antisera

Antisera directed against BrkA, OmpP, RmpM, FtsH, ZnuD, *E. coli* GroEL [13], *E. coli* BamA [40], and an antiserum directed against *E. coli* porin PhoE, which also cross-reacts with the other porins OmpF and OmpC [41], were used. Horseradish peroxidase-conjugated monoclonal antibodies directed against the FLAG tag were purchased from Sigma–Aldrich. To obtain antisera recognizing BB4107 and BP2019/BB1848, rabbits were immunized at GenScript (Piscataway, New Jersey, USA) with peptides CEGRAANRRVEVYLY and CKLSVRGLGAARPVQ, respectively. Peptides were chosen using the OptimumAntigen design tool. Additional antisera directed against BP2019/BB1848 were raised by immunizing two rabbits at Eurogentec (Liège, Belgium) with peptides CGHTDSKGSDSYNKGL and CARHEGVSVRQGKDAV. An N-terminal cysteine was included in each peptide for coupling of the peptide to carrier protein keyhole limpet hemocyanin before immunization.

2.6. SDS-PAGE and immunoblotting

Samples were mixed with sample buffer [42] with or without 25 mM dithiothreitol (DTT) replacing β-mercaptoethanol and either boiled or not before loading onto polyacrylamide gels. After electrophoresis, gels were stained with Bradford reagent [43] or silver to stain proteins (Pierce) or LPS [44]. Alternatively, proteins were transferred from the gels onto 0.45-μm pore-size nitrocellulose membranes (GE Healthcare). The membranes were incubated with the primary antisera described above and subsequently with horseradish peroxidase-conjugated goat anti-rabbit or anti-mouse IgG antisera (ThermoFisher) as appropriate. Antibody binding was detected with Clarity Western ECL Blotting Substrate (Bio-Rad).

2.7. Protease accessibility assay

Cell envelopes, isolated as described above, were incubated with 50 μg/mL of trypsin (Sigma–Aldrich) in 20 mM Tris–HCl (pH 8) for 15 min at 37 °C. Trypsin inhibitor (Boehringer Mannheim) was added to a final concentration of 33.3 μg/mL, and the suspension was cooled on ice. Cell envelopes were pelleted by centrifugation (30 min at 14,000×*g* and 4 °C) and processed for SDS-PAGE analysis.

2.8. Microscopy

To determine cell morphology, cells were fixed with 1% formaldehyde in PBS for 1 h at room temperature. Membranes were labeled with 5 μg/mL of the lipophilic dye FM 4–64 in PBS (Invitrogen), and cells were spotted on 1% agarose pads. Bacteria were visualized on a Zeiss Axioskop 2 fluorescence microscope with a 100x objective.

OMVs were visualized by transmission electron microscopy as previously described [13].

2.9. Dynamic light scattering (DLS)

The diameter of isolated OMVs was measured by DLS as previously described [45]. Briefly, samples were 10-fold diluted and measured in micro-volume cuvettes (Sarstedt) at 25 °C on a Zetasizer nano (Malvern Panalytical). Three technical replicates were performed per sample. Each technical replicate is an average of 10–20 measurements.

2.10. Determination of phosphatidylethanolamine (PE) at the cell surface

Cell-surface-exposed PE was detected with a PE-specific fluorescent probe consisting of FITC-PEG5000-NHS (PG2-FCNS-5k, Nanocs) coupled cinnamycin (BioAustralis) as described previously [46] (de Jonge et al., manuscript submitted for publication). Bacterial cells grown in SS medium were harvested at the specified time point, washed with PBS, and resuspended to an OD_{600} of 1 in PBS. Cells were then incubated with 0.5 μM of the PE probe for 30 min at 35 °C. After three washes with PBS, binding of the probe was measured as fluorescence intensity at 485 nm (excitation) and 528 nm (emission).

2.11. Susceptibility to SDS

Lysis induced by SDS was determined as previously described [47] (de Jonge et al., manuscript submitted for publication). Bacteria were grown in SS medium, harvested at the specified time point, washed with physiological salt solution and resuspended to an OD_{600} of 1. The bacterial suspensions were incubated with either 0 or 0.025% SDS for 5 min at room temperature, and the OD_{600} of the samples was measured.

2.12. Susceptibility to rifampicin

Bacteria grown until the specified time point were diluted to an OD_{600} of 0.05 in SS medium and grown for 16 h. The cultures were then diluted to an OD_{600} of 0.3 in fresh medium, and they were grown again for 8 h with either 0 or 0.25 μg/mL of rifampicin. The OD_{600} was monitored over time.

2.13. Multiple sequence alignment

Amino-acid sequences were aligned with Clustal Omega [48] and visualized using Jalview [49].

3. Results

3.1. Characterization of RmpM in bordetella

The OmpA-family protein encoded by locus tags BP0943 in *B. pertussis* strain Tohama I or BB3474 in *B. bronchiseptica* strain RB50 contains a PG-binding OmpA_C-like domain, but it does not contain an N-terminal β-barrel that could anchor it in the OM. It was therefore named RmpM after its *N. meningitidis* homologue, the reduction-modifiable protein M [13]. Like *N. meningitidis* RmpM, *Bordetella* RmpM contains two cysteines (see also Fig. 7A), which may form a disulfide bond, and might be responsible for a shift in electrophoretic mobility dependent on the absence or presence of a reducing agent in SDS-PAGE analysis. First, we verified the reduction modifiability of *B. pertussis* RmpM by SDS-PAGE. The electrophoretic mobility of RmpM shifted in the presence of the reducing agent DTT (Supplementary Fig. S1), showing that *B. pertussis* RmpM is indeed reduction modifiable.

To determine if RmpM may play a role in anchoring of the OM to the PG layer, we next analyzed if it, like *N. meningitidis* RmpM [50], interacts with the OM via the porins. The major porin in *B. pertussis* is OmpP and, like other Gram-negative bacterial porins, this protein forms oligomers, which do not dissociate when analyzed by SDS-PAGE under non-denaturing conditions, i.e. without boiling of the samples [51]. Accordingly, OmpP, which migrates as a protein with an apparent molecular weight of ~40 kDa in denatured samples, was detected in a ~90-kDa complex in the unheated samples (Fig. 1A, left panel). Under these non-denaturing conditions, RmpM, which migrates as a ~23-kDa protein in the heated samples, could be detected in a complex with the same apparent molecular weight as the OmpP complex, indicating that it is part of this complex (Fig. 1A, right panel). As the OmpA_C-like domain of RmpM is expected to extend into the periplasm to interact with the PG layer, it should be accessible to trypsin. Indeed, RmpM is degraded in the presence of trypsin (Fig. 1A, right panel). However, the integral membrane protein OmpP is not affected by trypsin, as confirmed by Western blot analysis under denaturing conditions (Fig. 1A, left panel). Nevertheless, the electrophoretic mobility of the high-molecular weight OmpP complex was increased after trypsin digestion (Fig. 1A, left panel), indicating that an interaction partner, presumably RmpM, was degraded. These results indicate that RmpM is associated with porin OmpP and could, therefore, form a link between the OM and the PG layer.

To increase OMV production in *B. pertussis* and *B. bronchiseptica*, we aimed at reducing the association of the OM with the PG layer by constructing *rmpM* mutants. Despite several attempts, deletion of *rmpM* was unsuccessful, presumably because RmpM is essential in *Bordetella* as suggested previously [52,53]. Therefore, we tried to create conditional *rmpM* mutants by inactivating *rmpM* in strains carrying a plasmid that contained a recombinant *rmpM* gene downstream of an IPTG-inducible promoter. The encoded RmpM protein, which carries a C-terminal FLAG tag, could already be detected in the absence of IPTG in *E. coli* strain BL21 (DE3) harboring plasmid pRmpM, and its expression increased in the presence of IPTG (Fig. 1B, left panels). Apart from the native RmpM, faster and slower migrating forms could be detected in the presence of IPTG, probably correlating with a degradation product and the unprocessed, signal-sequence-bearing precursor of RmpM, respectively. Remarkably, overproduction of RmpM reduced the abundance of porin OmpF in this strain (Fig. S2). Also in *B. pertussis* and *B. bronchiseptica* containing pRmpM, recombinant RmpM could be detected on Western blots with antibodies directed against the FLAG tag but only after growth of the bacteria with IPTG (Fig. 1B, upper right panel). With antiserum directed against RmpM, recombinant RmpM could only be detected in *B. pertussis* (Fig. 1B,

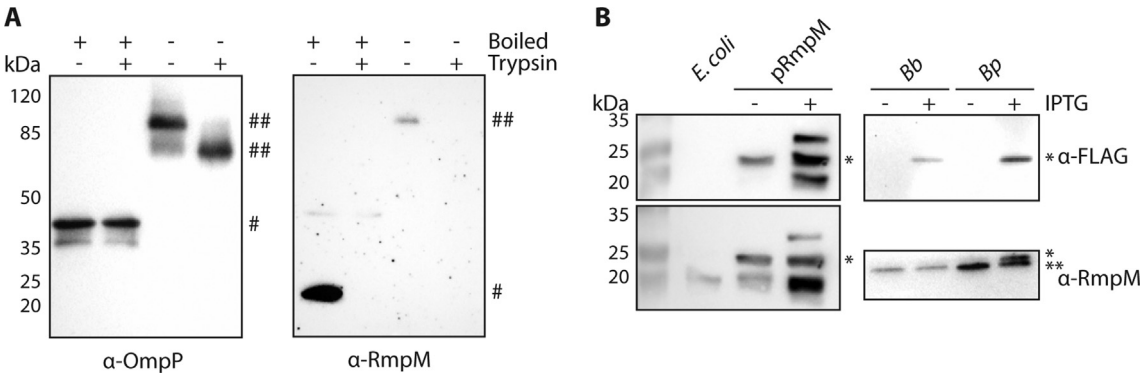

Fig. 1. Characterization of RmpM in *Bordetella*. (A) Cell envelopes of *B. pertussis* were either incubated with trypsin or not, and either boiled or not, in sample buffer before SDS-PAGE analysis as indicated in the figure. Membranes were incubated with antisera directed against OmpP (left panel) and RmpM (right panel). #, denatured monomeric OmpP or RmpM; ##, high-molecular-weight complexes. (B) Whole-cell lysates of *E. coli* strain BL21 (DE3) with or without pRmpM (left panels) and of *B. bronchiseptica* (*Bb*) and *B. pertussis* (*Bp*) with pRmpM (right panels) were analyzed by Western blotting using anti-FLAG tag antibodies and anti-RmpM antiserum. Strains harboring pRmpM were grown with (+) or without (−) IPTG. *, recombinant RmpM; **, chromosomally encoded native RmpM.

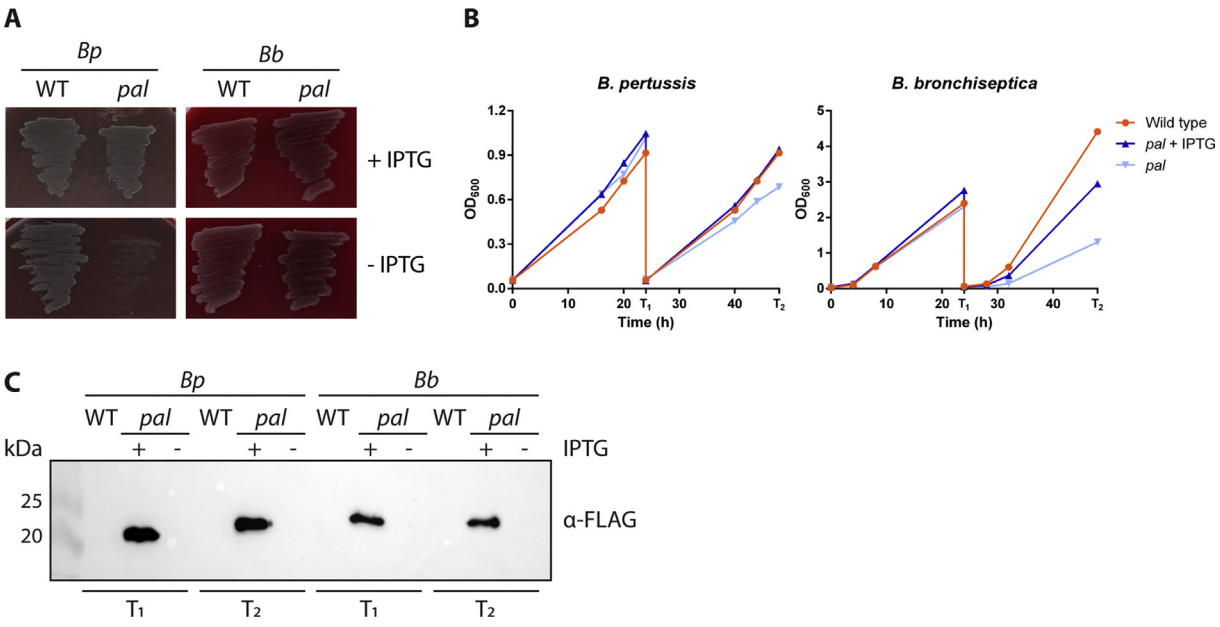

Fig. 2. Effect of Pal depletion on growth. (A) Wild-type (WT) *B. pertussis* (*Bp*) and *B. bronchiseptica* (*Bb*) and their Δ*pal* pPal derivatives (*pal*) were grown on BG agar plates either supplemented with IPTG or not. Growth of *B. pertussis* and *B. bronchiseptica* was assessed after 4 and 3 days of incubation at 35 °C, respectively. (B) Bacteria were pre-grown in SS medium supplemented, for the Δ*pal* pPal strains, with IPTG. After washing, the cells were diluted into fresh medium, which was, for the Δ*pal* pPal strains, either supplemented with IPTG or not, as indicated, and the OD_{600} was monitored in time. After 24 h of growth (T_1), cultures were again diluted into the same medium and grown for another 24 h (T_2). The graph is a representative of three independent experiments. (C) Cells were collected at T_1 and T_2, and the presence of recombinant Pal was analyzed by Western blotting using anti-FLAG tag antibodies. Equal amounts of cells were loaded on OD_{600} basis.

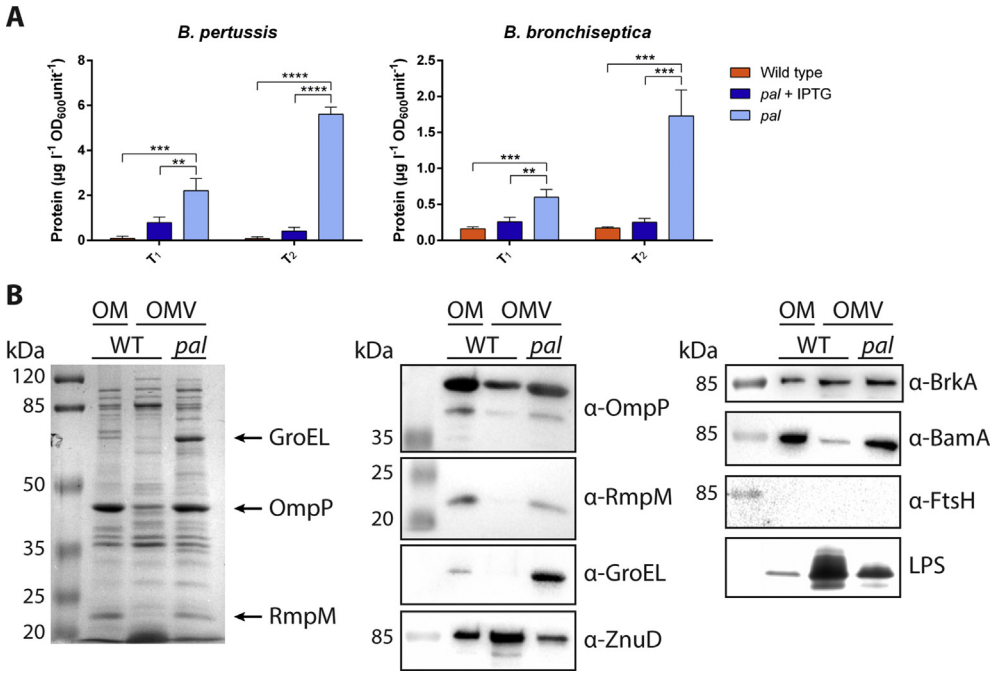

Fig. 3. OMV production under Pal-depletion conditions. Wild-type *B. pertussis* and *B. bronchiseptica* and the Δ*pal* pPal mutant derivatives (*pal*) were grown in SS medium either with or without IPTG. At T_1 and T_2 (where T_1 and T_2 are defined as in Fig. 2B), OMVs were isolated from culture supernatants. (A) OMV yield was determined based on protein content by Lowry assays and is expressed as the amount of protein per liter per OD_{600} unit. Bars represent mean values with standard deviations of three biological replicates. Significant differences were determined by one-way ANOVA followed by Tukey's multiple comparisons test using GraphPad Prism 6 (**, $p < 0.01$; ***, $p < 0.001$; ****, $p < 0.0001$). (B) The composition of OMVs from the Δ*pal* pPal mutant (*pal*) of *B. pertussis*, isolated at T_2 after growth without IPTG, was compared with a purified OM fraction and OMVs from the wild-type strain by SDS-PAGE analysis. Proteins were stained with the Bradford reagent (left panel). Specific proteins were detected by Western blotting using antisera directed against the proteins indicated in the figure (middle and right panels). Note that IM marker protein FtsH can be detected neither in the purified OM fraction nor in the isolated OMVs, but it can be detected in IM fractions ([13] and Fig. S4). LPS content was visualized by silver staining after SDS-PAGE analysis. Positions of molecular-weight marker proteins are indicated at the left of the panels.

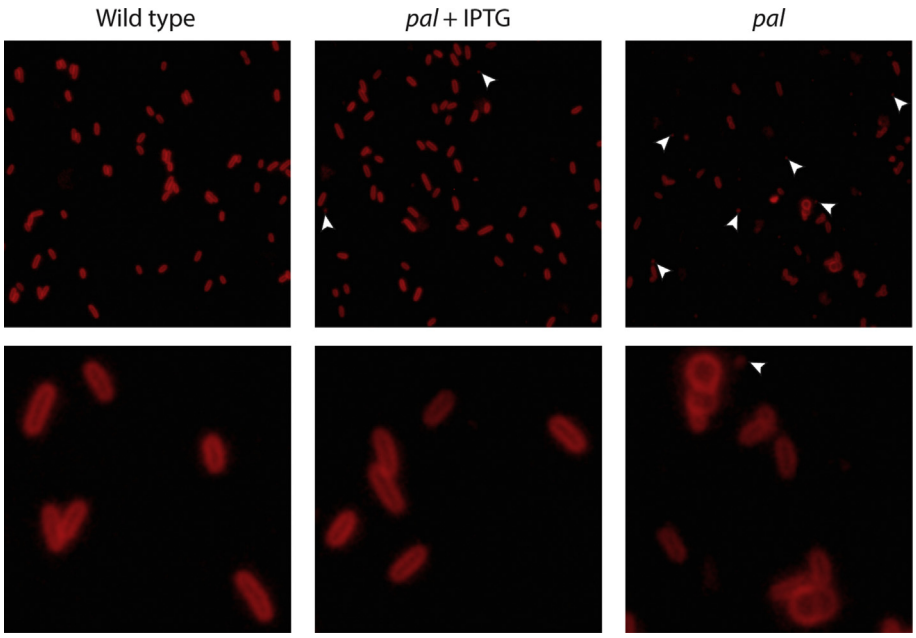

Fig. 4. Cell morphology. Wild-type *B. pertussis* and its Δ*pal* pPal mutant derivative (*pal*), grown with or without IPTG, were collected at T_2 (where T_2 is defined as in Fig. 2B), stained with the membrane dye FM 4–64, and visualized by fluorescence microscopy. Examples of possible OMVs are indicated by white arrowheads.

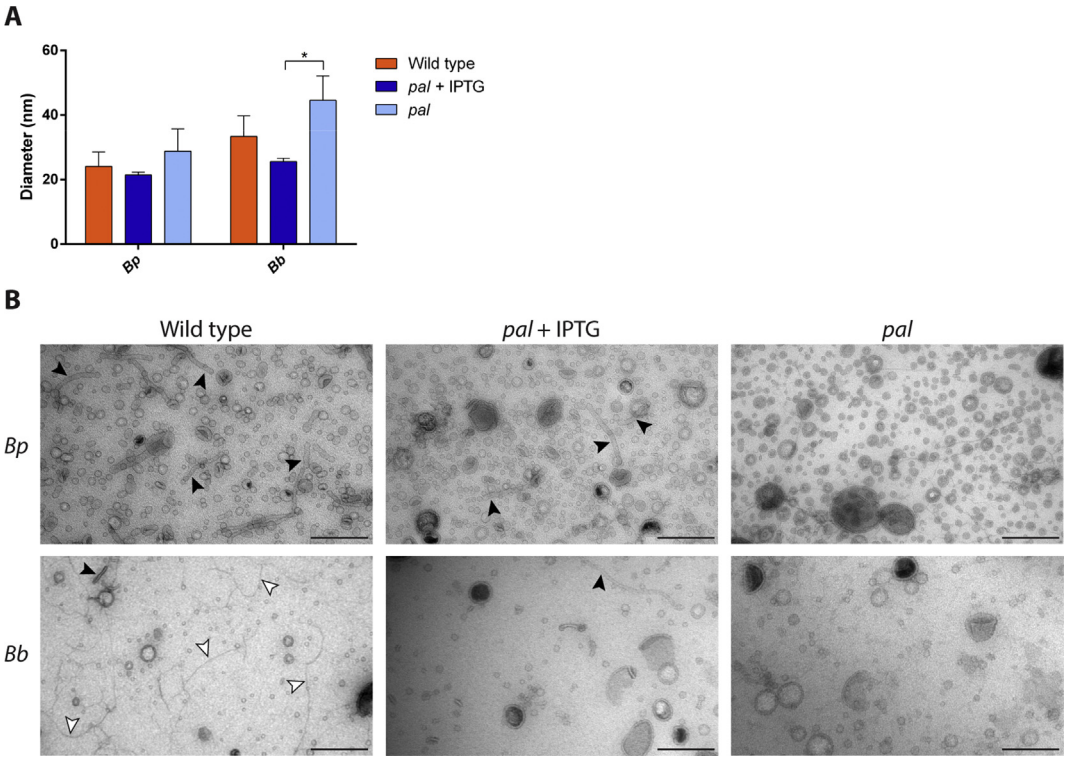

Fig. 5. Size of isolated OMVs. Wild-type *B. pertussis* and *B. bronchiseptica* and their Δ*pal* pPal (*pal*) derivatives were grown in SS medium with or without IPTG, and OMVs were isolated at T_2 (where T_2 is defined as in Fig. 2B). (A) The diameter of the OMVs was determined by DLS. Bars represent mean values with standard deviations of three independent experiments. Significant differences were determined by one-way ANOVA followed by Tukey's multiple comparisons test using GraphPad Prism 6 (*, $p < 0.05$). (B) OMVs were visualized by transmission electron microscopy. Scale bar equals 200 nm. Black and white arrowheads indicate observed tubular structures and putative flagella, respectively.

lower right panel) where the amount of recombinant RmpM produced appeared comparable to that of the chromosomally encoded native RmpM. We then tried to inactivate *rmpM* in the strains harboring pRmpM, but, unfortunately, this failed in either *Bordetella* species.

3.2. Construction of conditional pal mutants

As inactivation of *rmpM* failed, we chose a different approach to reduce the anchoring of the OM to the PG layer, i.e. by inactivating the *pal* gene. In addition, we targeted another gene coding for a

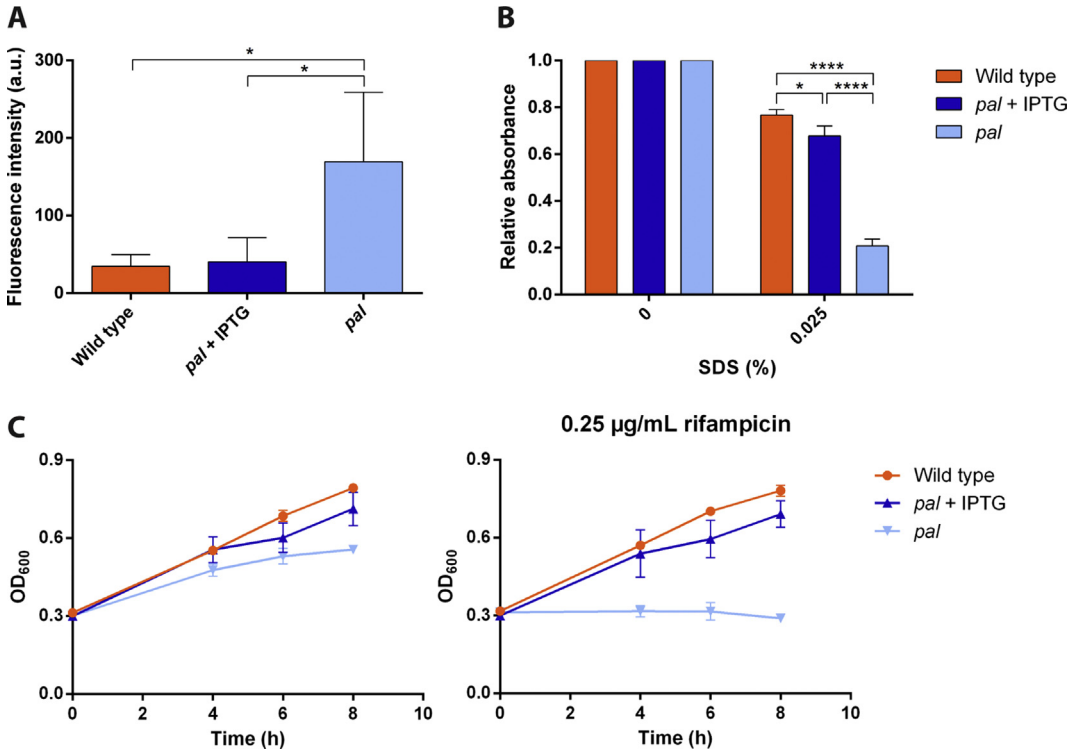

Fig. 6. Pal depletion disrupts OM lipid asymmetry in *B. pertussis*. (A,B) Wild-type *B. pertussis* and its Δ*pal* pPal mutant derivative (*pal*) were grown in SS medium with or without IPTG and harvested at T_2 (where T_2 is defined as in Fig. 2B). (A) The presence of PE at the cell surface was determined by incubating intact cells with a PE-specific fluorescent probe. Binding of the probe was measured as fluorescence intensity. (B) Bacteria were incubated with 0 or 0.025% SDS for 5 min. Cell lysis was determined by OD_{600} measurements. Values are expressed as OD_{600} of samples incubated with SDS relative to OD_{600} values after incubation without SDS. (C) Cultures grown in SS medium with or without IPTG were diluted at T_1 (where T_1 is defined as in Fig. 2B), grown for 16 h and diluted again in fresh medium. Cultures were then grown for 8 h either without (left panel) or with (right panel) rifampicin, and growth was monitored by OD_{600} measurements. Graphs show mean values and standard deviations of four (A) or three (B,C) independent experiments. (A,B) Significant differences were determined by one-way ANOVA followed by Tukey's multiple comparisons test using GraphPad Prism 6 (*, $p < 0.05$; ****, $p < 0.0001$).

component of the Tol-Pal system, i.e. *tolR*. Again, like for *rmpM*, repeated attempts to inactivate *tolR* and *pal* directly were unsuccessful, probably because they are essential for viability as suggested previously [52,53]. Hence, we aimed at constructing *pal* depletion strains. Indeed, we succeeded to inactivate chromosomal *pal* in *B. pertussis* and *B. bronchiseptica* strains harboring pPal, a plasmid containing *pal* with a 3' FLAG-tag-coding sequence under an IPTG-inducible promoter. To assess the growth of the recombinant strains under Pal-depletion conditions, wild-type *B. pertussis* and *B. bronchiseptica* and their Δ*pal* pPal derivatives were streaked on BG agar plates either containing IPTG or not. Growth of the *B. pertussis* Δ*pal* pPal strain, but not that of the *B. bronchiseptica* Δ*pal* pPal strain, was heavily compromised in the absence of IPTG (Fig. 2A). Both strains were viable on plates supplemented with IPTG. These results confirm that Pal is essential for the viability of *B. pertussis*. Leaky expression from the *tac* promoter could perhaps be sufficient to sustain growth of the *B. bronchiseptica* mutant in the absence of IPTG. Growth of the recombinant strains was further assessed in liquid medium. To this end, wild-type *B. pertussis* and *B. bronchiseptica* and the Δ*pal* pPal mutant derivatives were pre-grown in SS medium, which was supplemented with IPTG for the recombinant strains. After pre-growth, the cells were washed and diluted into fresh medium, either supplemented with IPTG or not. Growth of the wild-type and mutant strains was comparable during the first 24 h (Fig. 2B). Western blot analysis targeting the FLAG tag failed to detect the recombinant Pal after 24 h (time point T_1) in the Δ*pal* pPal mutants grown without IPTG, i.e. under Pal-depletion conditions (Fig. 2C). Cultures were subsequently diluted into fresh medium and grown for another 24 h (time point T_2). This resulted in a growth defect of the Δ*pal* pPal mutants in the absence of IPTG (Fig. 2B). In the case of *B. bronchiseptica*, the Δ*pal* pPal mutant grown with IPTG also exhibited some growth defect compared to the wild type, possibly because even induced *pal* expression from the plasmid is lower than chromosomal expression. Western blot analysis again failed to detect the FLAG-tagged Pal in the *pal* mutants grown without IPTG at time point T_2 (Fig. 2C). These results confirm that Pal is important to sustain normal growth.

3.3. Pal depletion results in hypervesiculation

To investigate the effect of Pal depletion on vesiculation in *B. pertussis* and *B. bronchiseptica*, strains were grown in Erlenmeyer flasks with an air:liquid ratio of 5:1, which results in efficient OMV production by *Bordetella* spp., as previously reported [13,54]. Cells were grown as above, and OMVs were isolated at time points T_1 and T_2. OMV production was quantified based on protein content, which indicated a significant increase in OMV production under Pal-depletion conditions at T_1 and T_2 relative to OMV production by the wild types or the Δ*pal* pPal mutant strains grown in medium supplemented with IPTG (Fig. 3A).

For potential vaccine application, it is important that relevant OM antigens are present in the OMVs. The composition of OMVs released by the Pal-depleted *B. pertussis* strain was compared with those of OMVs and a purified OM fraction of the wild-type strain. In accordance with previous results [13], OmpP and RmpM were much less abundant in OMVs from the wild-type strain than in the purified OM fraction (Fig. 3B, left and middle panel). Interestingly, their abundance was much higher in OMVs released by the Pal-

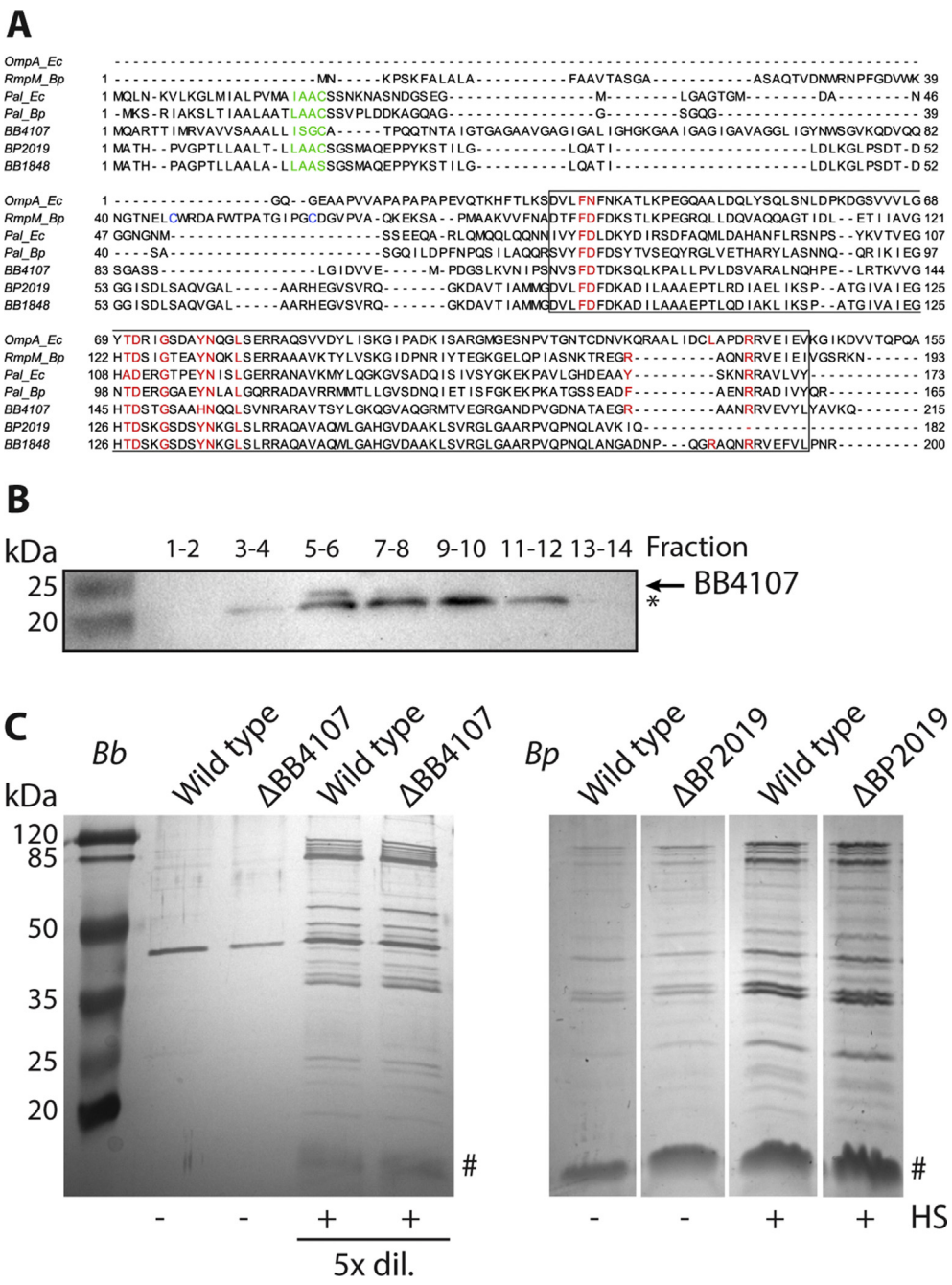

Fig. 7. Lipoproteins potentially involved in anchoring the OM to the PG layer. (A) Multiple sequence alignment of proteins with a PG-binding domain. The two cysteines of RmpM are indicated in blue. The OmpA_C-like domain is outlined in a black box. The lipobox and the PG-binding residues are indicated in green and red, respectively. Of OmpA, only the periplasmic domain is included in the alignment. *Ec*, *Escherichia coli*; *Bp*, *Bordetella pertussis*. (B) Cell envelopes of *B. bronchiseptica* were fractionated by isopycnic sucrose-density gradient centrifugation, and pooled fractions were analyzed by Western blotting using anti-BB4107 peptide antiserum. Pooled fraction 5/6 corresponds to an OM fraction as shown in Fig. S4. *, cross-reacting band. (C) Wild-type *B. bronchiseptica* (*Bb*) and *B. pertussis* (*Bp*) and their ΔBB4107- and ΔBP2019-mutant derivatives, respectively, were grown in Verwey medium and either inactivated by heat shock (HS) or not before OMV isolation, as indicated. Isolated OMVs were analyzed by SDS-PAGE, and gels were stained with silver (left panel) or with the Bradford reagent (right panel). Five-fold dilutions of the *Bb* OMVs obtained after HS were loaded compared to OMVs isolated without HS. LPS (lipid A plus core moiety) stained by both reagents, is indicated with #.

depleted strain and similar to that in the OM fraction (Fig. 3B, left and middle panels). Actually, the protein composition of the OMVs produced by Pal-depleted cells closely resembled that of the OM fraction, except for the presence of an abundant protein with an apparent molecular weight of ~65 kDa (Fig. 3B, left panel). Using Western blot analysis, we confirmed that this protein is the cytoplasmic chaperone GroEL (Fig. 3B, middle panel). The abundances of the zinc receptor ZnuD and the autotransporter BrkA were comparable in all samples (Fig. 3B, middle and right panels). Like porin OmpP and RmpM, the β-barrel assembly machinery component A (BamA) was more abundant in the OM fraction and in OMVs isolated from Pal-depleted bacteria than in OMVs from the wild-type cells. To examine if the OMV preparation was contaminated with IMs, which could happen as a consequence of cell lysis, we determined the presence of IM protein FtsH. However, FtsH could not be detected in any of the samples tested (Fig. 3B, right

panel). Probably due to the use of EDTA during the OM isolation procedure, the level of LPS in the OM fraction was lower than that in OMVs, with the highest amount of LPS in OMVs released by the wild-type strain (Fig. 3B, right panel). In conclusion, Pal depletion results in the increased release of OMVs with a protein composition very similar to that of the OM and deviant from that of OMVs released by wild-type cells.

3.4. Pal depletion affects cell morphology

To determine if Pal is involved in cell division in *B. pertussis*, Pal-depleted cells were stained with the fluorescent lipophilic dye FM 4–64 and visualized by microscopy. Cells of wild-type *B. pertussis* and of the Δ*pal* pPal mutant derivative grown with IPTG were mostly visible as individual coccobacilli (Fig. 4, left and middle panels). The Pal-depleted cells showed gross morphological changes, including large swollen cells (Fig. 4, right panels). Although no long chains of cells were observed, cell division seemed to be impaired as many pairs or small clusters of cells were detected. These results suggest a role for Pal in maintaining cell morphology. Besides, large spherical structures, which could represent OMVs, were detected, particularly in the Pal-depleted mutant, but also after growth of this strain in the presence of IPTG (indicated with arrowheads in Fig. 4). As the OMVs released from wild-type cells are rather small, i.e. in the range of 20–50 nm in diameter [13], we wondered if the diameter of OMVs released from Pal-depleted cells would be different. The average diameter of the isolated OMVs was determined by DLS and found to be similar between OMVs from the wild-type strain and the Pal-depleted strain of *B. pertussis* (Fig. 5A). A statistically significant difference in size was only observed between OMVs from the *B. bronchiseptica* Δ*pal* pPal mutant grown in the presence or absence of IPTG (Fig. 5A). Furthermore, OMVs were visualized by transmission electron microscopy. The majority of isolated OMVs was smaller than 50 nm (Fig. 5B), which corresponds to the DLS data. This was also the case for OMVs released by the Δ*pal* pPal mutant strains, although some larger vesicles (100–200 nm) were released as well, independent of the presence of IPTG. Besides spherical OMVs, also some tubular structures were visible (indicated with black arrowheads in Fig. 5B, left and middle panels), reminiscent of those released by *B. bronchiseptica* in the presence of the host defense peptide PMAP-36 [45], and similar structures have also been described in the first study ever reporting about *B. pertussis* OMVs in 1970 [55]. In the OMV preparation from wild-type *B. bronchiseptica*, thinner structures were noticeable that are, presumably, flagella (indicated with white arrowheads in Fig. 5B, lower left panel). In conclusion, although some larger OMVs might be released by the Δ*pal* pPal strain, the majority is of the same small size as those released by the wild-type strain.

3.5. Pal is important for maintaining the OM barrier function

Apart from its structural role and its role in cell division, the Tol-Pal system has been reported to be involved in maintaining the lipid asymmetry of the OM in *E. coli* and *S.* Typhimurium by mediating retrograde phospholipid transport [34,56]. To determine the effect of Pal depletion on OM lipid asymmetry, the binding of a large, membrane-impermeable, PE-specific fluorescent probe to intact bacterial cells was studied. Binding of the PE-specific probe was significantly increased in Pal-depleted *B. pertussis* cells (Fig. 6A). This result suggests that the Tol-Pal system is required for maintaining OM lipid asymmetry in *B. pertussis*, possible by mediating retrograde phospholipid transport. However, a limitation of the assay is that we cannot totally exclude the possibility that the OM is damaged to such an extent that even this very large probe (>5 kDa) can pass and reach the inner membrane.

The asymmetric OM of Gram-negative bacteria forms a barrier against detrimental compounds in the environment, such as antibiotics, detergents, and bile salts [57]. The increased presence of phospholipids at the cell-surface in the Pal-depleted cells will create phospholipid-bilayer patches, which is expected to lead to increased susceptibility to hydrophobic noxious compounds. To test this possibility, SDS-mediated cell lysis of wild-type *B. pertussis* and its mutant derivative was determined. Cell lysis was significantly higher in the Pal-depleted cells (Fig. 6B). Furthermore, susceptibility to rifampicin, a hydrophobic antibiotic that diffuses through the OM via phospholipid bilayer patches [58], was determined. Cultures were adjusted to a similar OD_{600} and grown in the absence or presence of rifampicin. Growth of the wild-type strain and the Δ*pal* pPal mutant supplemented with IPTG was not affected by rifampicin (Fig. 6C). However, without IPTG, the Δ*pal* pPal cells were unable to grow in the presence of rifampicin. Together, these results indicate that Pal depletion disrupts the barrier function of the OM in *B. pertussis*.

3.6. Identification of proteins with a putative PG-binding C-terminus

Searching the genome sequences of *B. pertussis* Tohama I and *B. bronchiseptica* RB50 with BLASTp identified two additional proteins containing an OmpA_C-like domain, i.e. BP2019/BB1848 and BB4107, which has no homologue in *B. pertussis*. As these proteins contain the residues within the OmpA_C-like domain that bind PG (Fig. 7A) [59], they are potentially also involved in anchoring the OM to the PG layer. Based on the presence of a lipobox motif (Fig. 7A), BP2019 and BB4107 are lipoproteins, and they are probably anchored to the OM via their lipid moieties. Remarkably, BB1848, the homologue of BP2019, is probably not a lipoprotein as the canonical cysteine at the fourth position of the lipobox motif is lacking (Fig. 7A). This residue, which is the first residue of the mature protein after cleavage of the signal sequence, is essential for lipidation [60].

Next, we wished to determine the subcellular localization of these proteins. To facilitate their detection, antisera were raised against BB4107 and BP2019/BB1848 peptides. Although many cross-reacting bands were detected by Western blotting of cell lysates, the BB4107-specific band could be identified by its absence in the lysate of the constructed ΔBB4107-mutant strain (Fig. S3A). After cell lysis, the protein fractionated with the cell envelopes (Fig. S3B, lanes 1 and 2). IM and OM were then separated via isopycnic sucrose-gradient density centrifugation, and IM marker FtsH and OM marker RmpM were found to be most abundant in fractions 2–4 and 5–7, respectively (Fig. S4). Fractions were then pooled and BB4107 was found to be present mostly in pooled fraction 5/6 (Fig. 7B), indicating that BB4107 is localized in the OM. The observation that the protein is extractable from the cell envelopes with sarkosyl (Fig. S3B, lanes 3 and 4) is in agreement with the notion that the protein is not an integral OM protein but is anchored to the OM via its lipid moiety. BP2019 and BB1848 could not be detected with three antisera obtained after immunization of rabbits with, in total, three different peptides (data not shown), suggesting that their abundance is low in both species. Next, we investigated if inactivation of BP2019 in *B. pertussis* or BB4107 in *B. bronchiseptica* could improve OMV production. However, similar amounts of OMVs were isolated from the mutants as from the wild-type strains (Fig. 7C). We previously showed that applying a heat shock to bacterial cells results in increased OMV release [13]. Also after applying a heat shock, OMV production in the BP2019 and

BB4107 mutant strains was similar as in the corresponding wild types (Fig. 7C).

4. Discussion

New generation vaccines for *B. pertussis* and *B. bronchiseptica* could be based on OMVs, but, unfortunately, spontaneous vesiculation by bordetellae is relatively low. To improve vesiculation, we aimed in this study at reducing the links between the OM and the PG layer.

Initially, we focused on RmpM, which has a PG-binding OmpA_C-like domain. We previously showed that *B. pertussis* OMVs are depleted of RmpM suggesting they arise at sites in the OM where the abundance of RmpM is low [13]. RmpM of *N. meningitidis* and its homologue PapA of *Comamonas testosteroni* are associated with the OM by interacting with the porins [50,61]. The observation that *B. pertussis* OMVs are depleted not only of RmpM, but also of porin OmpP [13] indicated that RmpM is probably also associated with porins in *B. pertussis*. In the current study, we provide biochemical evidence for the presumed association between RmpM and OmpP (Fig. 1A), which shows that indeed RmpM could form a link between the OM and the PG layer. Therefore, to increase OMV production, *rmpM* was targeted by mutagenesis but despite frequent attempts, we were not able to construct *rmpM* mutants, possibly because the gene is essential for viability as suggested previously [52,53]. Attempts to construct conditional *rmpM* mutants also failed, possibly because of a polar effect of the mutation on downstream gene BP0942, coding for a ubiquinone biosynthesis O-methyltransferase, which was also classified as essential [52,53]. RmpM remains an interesting target for mutagenesis in order to increase OMV production in *Bordetella*. Besides its role in anchoring the OM to the PG layer, RmpM of *N. meningitidis* also stabilizes porin trimers and the Bam complex. The N-terminal part of RmpM is sufficient for this stabilization [62]. Possibly, the N-terminal domain of *B. pertussis* RmpM has a similar role in stabilizing OM protein complexes and then, it could be that only this domain is essential for viability. If that is the case, mutant strains could be constructed that only express the N-terminal segment of RmpM, thereby maintaining the association of RmpM with OM proteins. The lack of the C-terminal PG-binding domain is expected then to result in decreased anchoring of the OM to the PG layer and in increased OMV production.

Since the construction of *rmpM* mutants failed, we switched focus to Pal. In other bacteria, such as *E. coli*, *S.* Typhimurium and *H. pylori*, *tol-pal* mutants could be constructed, and such mutants are hypervesiculating [34–36,47,63]. No homologues of the Tol-Pal system can be found by BLASTp searches in the pathogenic *Neisseriae*, *N. meningitidis* and *Neisseria gonorrhoeae*, which, like bordetellae, are β-proteobacteria. Therefore, we expected that the construction of *tolR* and *pal* mutants would be feasible, but this turned out not to be the case. In accordance with this result, the genes for the Tol-Pal system have previously been suggested to be essential in *Bordetella* [52,53]. However, we were able to construct conditional *pal* mutants.

Pal depletion resulted in increased OMV production. In *tol-pal* mutants of other bacteria, large OMVs are often formed at the division sites [31,47], which is probably related to the role of the Tol-Pal system in cell division. In *B. pertussis* and *B. bronchiseptica*, however, the majority of OMVs released from Pal-depleted cells were 20–50 nm in diameter (Fig. 5A), which is relatively small and not deviant from OMVs released from wild-type cells. The release of small OMVs may be advantageous for vaccine development, since it is easier for small OMVs to reach the periphery and be taken up by antigen-presenting cells.

The protein composition of OMVs from Pal-depleted cells was deviant from those of the wild-type strain, suggesting that they are released via different mechanisms. As discussed above, OMVs of wild-type *B. pertussis* are depleted of RmpM and OmpP, suggesting that OMVs are formed in areas of the OM where RmpM-mediated linkages to the PG are absent. Interestingly, also the BamA levels in these OMVs were relatively low (Fig. 3B), which can be explained if RmpM also interacts with BamA as has been demonstrated in *Neisseria meningitis* [62]. Thus, like in *N. meningitidis*, RmpM may be part of the Bam complex in *B. pertussis*. The presence of RmpM and associated OM proteins in the OMVs from the Pal-depleted cells suggests that the interaction between RmpM and the PG layer is weakened in the absence of Pal. In *E. coli*, Pal is known to interact with OmpA [64,65]. If Pal similarly interacts with RmpM in *B. pertussis*, the loss of Pal might affect the interaction of RmpM with PG.

In contrast to the OMVs of wild-type cells, the protein content of OMVs from Pal-depleted bacteria closely resembled that of the OM of *B. pertussis* (Fig. 3B). The most striking difference was the high abundance of GroEL in these OMVs. Although GroEL is a cytoplasmic chaperone, it is well known as a surface moonlighting protein with virulence functions in various bacteria [66]. GroEL has also been detected as an abundant protein on the surface of OMVs from *E. coli* cells that were stressed by the overproduction of the autotransporter Hbp [67]. Probably, the Pal-depleted *B. pertussis* cells are also stressed, and stress stimulates the release of GroEL from the cytoplasm and its appearance at the surface. GroEL has also been detected previously at the cell surface of *B. pertussis* [68], and interestingly, *in-vivo* studies in mice showed some protection to *B. pertussis* infection after immunization with GroEL [69].

Depletion of Pal altered cell morphology. In *S.* Typhimurium, *E. coli* and *Pseudomonas aeruginosa*, mutations in the Tol-Pal system often result in cell chaining [31,34,47,70], although this phenotype was shown to be dependent on the osmolarity of the medium in *E. coli* [31,71,72]. Although pairs and small clusters of cells were observed, no long chains of cells were detected in Pal-depleted *B. pertussis*, suggesting that the role of the Tol-Pal system in cell division might be somewhat different in this coccobacillus.

The lipid asymmetry of the OM appeared to be disrupted in Pal-depleted *B. pertussis* as manifested by increased amounts of PE at the cell surface and increased susceptibility to SDS and rifampicin. We have previously shown that the Mla system together with OM phospholipase A (OMPLA) plays a major role in maintaining lipid asymmetry in the OM (de Jonge et al., manuscript submitted for publication). The results presented here indicate that the Tol-Pal system also contributes to this process, as has been reported before in *E. coli* and *S.* Typhimurium [34,56]. It was suggested that the Tol-Pal system, like the Mla system, transports phospholipids in a retrograde direction from the OM to the IM [56]. Perhaps as a consequence of the defective retrograde transport of phospholipids and their resulting accumulation in the OM, the amount of LPS in the OMVs of the Pal-depleted cells appeared to be reduced as compared to that in wild-type OMVs (Fig. 3B). This reduced LPS content may be favorable for vaccine applications as it will reduce the endotoxicity of the OMVs.

The accumulation of phospholipids at the cell surface in Pal-depleted bacteria is expected to activate OMPLA which will lead to the release of free fatty acids. As fatty acids inhibit the growth of *B. pertussis* [73], the activation of OMPLA may explain our inability to obtain clean *tol-pal* mutants in this species. As *B. bronchiseptica* has a functional efflux pump, it is less susceptible to fatty acids [74]. Indeed, the growth of the Pal-depletion strain of this species on agar plates was clearly less dependent on the presence of IPTG than that of the *B. pertussis* mutant (Fig. 2A). Nevertheless, clean

knockouts could also not be obtained in this organism. It will be interesting to determine whether *tol-pal* mutants can be constructed in a mutant strain defective in *pldA*, the structural gene for OMPLA. Previously, we have demonstrated that a *B. pertussis* mutant lacking the Mla system shows a conditional growth defect and can be rescued either by a *pldA* mutation or by supplementation of the medium with starch (de Jonge et al., manuscript submitted for publication), which is known to absorb free fatty acids [75]. The SS medium used in the current study was supplemented with heptakis, which also protects *B. pertussis* against autoinhibition of growth by adsorbing free fatty acids [73], perhaps explaining the still considerable growth of Pal-depleted cells observed in our growth assays (Fig. 2B).

Besides RmpM and Pal, we identified several other proteins in *B. pertussis* and *B. bronchiseptica* with a high sequence similarity to the OmpA_C domain. Cell fractionation showed that BB4107 is localized in the OM, presumably by its lipid moiety, and, therefore, it could play a role in anchoring the OM to the PG layer. However, inactivation of BB4107 did not improve OMV production. We were unable to detect BP2019 and BB1848 by Western blot analysis using multiple antisera raised against various peptides of these proteins. This is probably due to the low expression of these genes [76,77]. Also in proteomic analyses of OMVs and whole cells of *B. pertussis*, BP2019 was not detected [78,79]. Furthermore, inactivation of BP2019 did not impact vesiculation, which is not surprising if, indeed, the expression level is low.

In conclusion, the hypervesiculating phenotype makes the conditional *pal* mutants potential candidates for the development of novel OMV-based *Bordetella* vaccines. We have previously described two other strategies to increase OMV production, i.e. by applying a heat shock to the bacterial cells [13] and by mutations in both the *mla* and *pldA* genes (de Jonge et al., manuscript submitted for publication). The protein compositions of spontaneous and heat-induced OMVs released from wild type strains [13] and of OMVs produced by the *B. pertussis mlaF pldA* mutant are comparable (de Jonge et al., manuscript submitted for publication). However, the composition of OMVs from Pal-depleted cells is different and more closely resembles the composition of the OM. This difference may result in differences in induced immunity. In future immunization experiments, the immune responses and the protection induced by the different OMV preparations need to be determined.

Declaration of competing interest

The authors declare no conflict of interests.

Acknowledgments

We would like to thank Nathalie Devos (GlaxoSmithKline Biologicals SA) for providing BrkA antiserum. We also thank Gosse Metz and Puck Roos for their contributions in initial experiments. This work received funding from the domain Applied and Engineering Sciences (TTW) of The Netherlands Organization for Scientific Research (NWO) (TTW Perspectief grant numbers 14921 and 14924), which received financial contributions for this grant from GlaxoSmithKline Biologicals SA and PULIKE Biological Engineering Inc.

Appendix A. Supplementary data

Supplementary data to this article can be found online at https://doi.org/10.1016/j.resmic.2022.103937.

References

[1] Cherry JD. Pertussis: challenges today and for the future. PLoS Pathog 2013;9:e1003418. https://doi.org/10.1371/journal.ppat.1003418.
[2] Geurtsen J, Steeghs L, Hamstra HJ, ten Hove J, de Haan A, Kuipers B, et al. Expression of the lipopolysaccharide-modifying enzymes PagP and PagL modulates the endotoxic activity of *Bordetella pertussis*. Infect Immun 2006;74:5574–85. https://doi.org/10.1128/IAI.00834-06.
[3] Cody CL, Baraff LJ, Cherry JD, Marcy SM, Manclark CR. Nature and rates of adverse reactions associated with DTP and DT immunizations in infants and children. Pediatrics 1981;68:650–60. https://doi.org/10.3390/ma4101861.
[4] Sato Y, Kimura M, Fukumi H. Development of a pertussis component vaccine in Japan. Lancet 1984;323:122–6. https://doi.org/10.1016/S0140-6736(84)90061-8.
[5] Cherry JD. The 112-year odyssey of pertussis and pertussis vaccines—mistakes made and implications for the future. J Pediatr Infect Dis Soc 2019. https://doi.org/10.1093/jpids/piz005.
[6] Mooi FR, van der Maas NAT, de Melker HE. Pertussis resurgence: waning immunity and pathogen adaptation - two sides of the same coin. Epidemiol Infect 2014;142:685–94. https://doi.org/10.1017/S0950268813000071.
[7] Warfel JM, Zimmerman LI, Merkel TJ. Acellular pertussis vaccines protect against disease but fail to prevent infection and transmission in a nonhuman primate model. Proc Natl Acad Sci Unit States Am 2014;111:787–92. https://doi.org/10.1073/pnas.1314688110.
[8] Ellis JA. How well do vaccines for *Bordetella bronchiseptica* work in dogs? A critical review of the literature 1977–2014. Vet J 2015;204:5–16. https://doi.org/10.1016/j.tvjl.2015.02.006.
[9] van der Pol L, Stork M, van der Ley P. Outer membrane vesicles as platform vaccine technology. Biotechnol J 2015;10:1689–706. https://doi.org/10.1002/biot.201400395.
[10] Raeven RHM, Brummelman J, Pennings JLA, van der Maas L, Tilstra W, Helm K, et al. *Bordetella pertussis* outer membrane vesicle vaccine confers equal efficacy in mice with milder inflammatory responses compared to a whole-cell vaccine. Sci Rep 2016;6:38240. https://doi.org/10.1038/srep38240.
[11] Raeven RHM, van Vlies N, Salverda MLM, van der Maas L, Uittenbogaard JP, Bindels THE, et al. The role of virulence proteins in protection conferred by bordetella pertussis outer membrane vesicle vaccines. Vaccines 2020;8:1–22. https://doi.org/10.3390/vaccines8030429.
[12] Hozbor D, Rodriguez ME, Fernández J, Lagares A, Guiso N, Yantorno O. Release of outer membrane vesicles from *Bordetella pertussis*. Curr Microbiol 1999;38:273–8. https://doi.org/10.1007/PL00006801.
[13] de Jonge EF, Balhuizen MD, van Boxtel R, Wu J, Haagsman HP, Tommassen J. Heat shock enhances outer-membrane vesicle release in *Bordetella* spp. Curr Res Microb Sci 2021;2:100009. https://doi.org/10.1016/j.crmicr.2020.100009.
[14] Powers MJ, Trent MS. Intermembrane transport: glycerophospholipid homeostasis of the Gram-negative cell envelope. Proc Natl Acad Sci Unit States Am 2019;116:17147–55. https://doi.org/10.1073/pnas.1902026116.
[15] Asmar AT, Collet J-F. Lpp, the Braun lipoprotein, turns 50—major achievements and remaining issues. FEMS Microbiol Lett 2018;365:fny199. https://doi.org/10.1093/femsle/fny199.
[16] Braun V, Rehn K. Chemical characterization, spatial distribution and function of a lipoprotein (murein-lipoprotein) of the *E. coli* cell wall: the specific effect of trypsin on the membrane structure. Eur J Biochem 1969;10:426–38. https://doi.org/10.1111/j.1432-1033.1969.tb00707.x.
[17] Braun V. Covalent lipoprotein from the outer membrane of *Escherichia coli*. Biochim Biophys Acta 1975;415:335–77. https://doi.org/10.1016/0304-4157(75)90013-1.
[18] Braun V, Bosch V. Sequence of the murein · lipoprotein and the attachment site of the lipid. Eur J Biochem 1972;28:51–69. https://doi.org/10.1111/j.1432-1033.1972.tb01883.x.
[19] Suzuki H, Nishimura Y, Yasuda S, Nishimura A, Yamada M, Hirota Y. Murein-lipoprotein of *Escherichia coli*: a protein involved in the stabilization of bacterial cell envelope. Mol Gen Genet 1978;167:1–9. https://doi.org/10.1007/BF00270315.
[20] Wang Y. The function of OmpA in *Escherichia coli*. Biochem Biophys Res Commun 2002;292:396–401. https://doi.org/10.1006/bbrc.2002.6657.
[21] De Mot R, Vanderleyden J. The C-terminal sequence conservation between OmpA-related outer membrane proteins and MotB suggests a common function in both Gram-positive and Gram-negative bacteria, possibly in the interaction of these domains with peptidoglycan. Mol Microbiol 1994;12:333–4. https://doi.org/10.1111/j.1365-2958.1994.tb01021.x.
[22] Arora A, Abildgaard F, Bushweller JH, Tamm LK. Structure of outer membrane protein A transmembrane domain by NMR spectroscopy. Nat Struct Biol 2001;8:334–8. https://doi.org/10.1038/86214.
[23] Ishida H, Garcia-Herrero A, Vogel HJ. The periplasmic domain of *Escherichia coli* outer membrane protein A can undergo a localized temperature dependent structural transition. Biochim Biophys Acta 2014;1838:3014–24. https://doi.org/10.1016/j.bbamem.2014.08.008.
[24] Sonntag I, Schwarz H, Hirota Y, Henning U. Cell envelope and shape of *Escherichia coli*: multiple mutants missing the outer membrane lipoprotein and other major outer membrane proteins. J Bacteriol 1978;136:280–5. https://doi.org/10.1128/jb.136.1.280-285.1978.

[25] Grizot S, Buchanan SK. Structure of the OmpA-like domain of RmpM from *Neisseria meningitidis*. Mol Microbiol 2004;51:1027–37. https://doi.org/10.1111/j.1365-2958.2003.03903.x.
[26] Steeghs L, Berns M, ten Hove J, de Jong A, Roholl P, van Alphen L, et al. Expression of foreign LpxA acyltransferases in *Neisseria meningitidis* results in modified lipid A with reduced toxicity and retained adjuvant activity. Cell Microbiol 2002;4:599–611. https://doi.org/10.1046/j.1462-5822.2002.00214.x.
[27] Klugman KP, Gotschlich EC, Blake MS. Sequence of the structural gene (*rmpM*) for the class 4 outer membrane protein of *Neisseria meningitidis*, homology of the protein to gonococcal protein III and *Escherichia coli* OmpA, and construction of meningococcal strains that lack class 4 protein. Infect Immun 1989;57:2066–71. https://doi.org/10.1128/iai.57.7.2066-2071.1989.
[28] Maharjan S, Saleem M, Feavers IM, Wheeler JX, Care R, Derrick JP. Dissection of the function of the RmpM periplasmic protein from *Neisseria meningitidis*. Microbiology 2016;162:364–75. https://doi.org/10.1099/mic.0.000227.
[29] van de Waterbeemd B, Streefland M, van der Ley P, Zomer B, van Dijken H, Martens D, et al. Improved OMV vaccine against *Neisseria meningitidis* using genetically engineered strains and a detergent-free purification process. Vaccine 2010;28:4810–6. https://doi.org/10.1016/j.vaccine.2010.04.082.
[30] Szczepaniak J, Press C, Kleanthous C. The multifarious roles of Tol-Pal in Gram-negative bacteria. FEMS Microbiol Rev 2020;44:490–506. https://doi.org/10.1093/femsre/fuaa018.
[31] Gerding MA, Ogata Y, Pecora ND, Niki H, de Boer PAJ. The *trans*-envelope Tol-Pal complex is part of the cell division machinery and required for proper outer-membrane invagination during cell constriction in *E. coli*. Mol Microbiol 2007;63:1008–25. https://doi.org/10.1111/j.1365-2958.2006.05571.x.
[32] Lloubès R, Cascales E, Walburger A, Bouveret E, Lazdunski C, Bernadac A, et al. The Tol-Pal proteins of the *Escherichia coli* cell envelope: an energized system required for outer membrane integrity? Res Microbiol 2001;152:523–9. https://doi.org/10.1016/S0923-2508(01)01226-8.
[33] Bouveret E, Derouiche R, Rigal A, Lloubès R, Lazdunski C, Bénédetti H. Peptidoglycan-associated lipoprotein-TolB interaction. J Biol Chem 1995;270:11071–7. https://doi.org/10.1074/jbc.270.19.11071.
[34] Masilamani R, Cian MB, Dalebroux ZD. *Salmonella* Tol-Pal reduces outer membrane glycerophospholipid levels for envelope homeostasis and survival during bacteremia. Infect Immun 2018;86:e00173-18. https://doi.org/10.1128/IAI.00173-18.
[35] Turner L, Praszkier J, Hutton ML, Steer D, Ramm G, Kaparakis-Liaskos M, et al. Increased outer membrane vesicle formation in a *Helicobacter pylori tolB* mutant. Helicobacter 2015;20:269–83. https://doi.org/10.1111/hel.12196.
[36] Bernadac A, Gavioli M, Lazzaroni JC, Raina S, Lloubès R. *Escherichia coli tol-pal* mutants form outer membrane vesicles. J Bacteriol 1998;180:4872–8. https://doi.org/10.1128/jb.180.18.4872-4878.1998.
[37] Verwey WF, Thiele EH, Sage DN, Schuchardt LF. A simplified liquid culture medium for the growth of *Hemophilus pertussis*. J Bacteriol 1949;58:127–34.
[38] Stainer DW, Scholte MJ. A simple chemically defined medium for the production of phase I *Bordetella pertussis*. J Gen Microbiol 1971;63:211–20. https://doi.org/10.1099/00221287-63-2-211.
[39] Paltansing S, Kraakman M, van Boxtel R, Kors I, Wessels E, Goessens W, et al. Increased expression levels of chromosomal AmpC β-lactamase in clinical *Escherichia coli* isolates and their effect on susceptibility to extended-spectrum cephalosporins. Microb Drug Resist 2015;21:7–16. https://doi.org/10.1089/mdr.2014.0108.
[40] Robert V, Volokhina EB, Senf F, Bos MP, van Gelder P, Tommassen J. Assembly factor Omp85 recognizes its outer membrane protein substrates by a species-specific C-terminal motif. PLoS Biol 2006;4:e377. https://doi.org/10.1371/journal.pbio.0040377.
[41] Goessens WHF, van der Bij AK, van Boxtel R, Pitout JDD, van Ulsen P, Melles DC, et al. Antibiotic trapping by plasmid-encoded CMY-2 β-lactamase combined with reduced outer membrane permeability as a mechanism of carbapenem resistance in *Escherichia coli*. Antimicrob Agents Chemother 2013;57:3941–9. https://doi.org/10.1128/AAC.02459-12.
[42] Laemmli U. Cleavage of structural proteins during the assembly of the head of bacteriophage T4. Nature 1970;227:680–5. https://doi.org/10.1038/227680a0.
[43] Bos MP, Tommassen-van Boxtel R, Tommassen J. Experimental methods for studying the BAM complex in *Neisseria meningitidis*. Methods Mol Biol 2015;1329:33–49. https://doi.org/10.1007/978-1-4939-2871-2_3.
[44] Tsai CM, Frasch CE. A sensitive silver stain for detecting lipopolysaccharides in polyacrylamide gels. Anal Biochem 1982;119:115–9. https://doi.org/10.1016/0003-2697(82)90673-X.
[45] Balhuizen MD, Versluis CM, van Harten RM, de Jonge EF, Brouwers JF, van de Lest CHA, et al. PMAP-36 reduces the innate immune response induced by *Bordetella bronchiseptica*-derived outer membrane vesicles. Curr Res Microb Sci 2021;2:100010. https://doi.org/10.1016/j.crmicr.2020.100010.
[46] Lin Y, Bogdanov M, Lu S, Guan Z, Margolin W, Weiss J, et al. The phospholipid-repair system LplT/Aas in Gram-negative bacteria protects the bacterial membrane envelope from host phospholipase A_2 attack. J Biol Chem 2018;293:3386–98. https://doi.org/10.1074/jbc.RA117.001231.
[47] Lo Sciuto A, Fernández-Piñar R, Bertuccini L, Iosi F, Superti F, Imperi F. The periplasmic protein TolB as a potential drug target in *Pseudomonas aeruginosa*. PLoS One 2014;9:e103784. https://doi.org/10.1371/journal.pone.0103784.
[48] Sievers F, Wilm A, Dineen D, Gibson TJ, Karplus K, Li W, et al. Fast, scalable generation of high-quality protein multiple sequence alignments using Clustal Omega. Mol Syst Biol 2011;7:539. https://doi.org/10.1038/msb.2011.75.
[49] Waterhouse AM, Procter JB, Martin DMA, Clamp M, Barton GJ. Jalview Version 2-a multiple sequence alignment editor and analysis workbench. Bioinformatics 2009;25:1189–91. https://doi.org/10.1093/bioinformatics/btp033.
[50] Jansen C, Wiese A, Reubsaet L, Dekker N, de Cock H, Seydel U, et al. Biochemical and biophysical characterization of in vitro folded outer membrane porin PorA of *Neisseria meningitidis*. Biochim Biophys Acta 2000;1464:284–98. https://doi.org/10.1016/S0005-2736(00)00155-3.
[51] Armstrong SK, Parr TR, Parker CD, Hancock REW. *Bordetella pertussis* major outer membrane porin protein forms small, anion-selective channels in lipid bilayer membranes. J Bacteriol 1986;166:212–6. https://doi.org/10.1128/jb.166.1.212-216.1986.
[52] Gonyar LA, Gelbach PE, McDuffie DG, Koeppel AF, Chen Q, Lee G, et al. *In vivo* gene essentiality and metabolism in *Bordetella pertussis*. mSphere 2019;4. https://doi.org/10.1128/msphere.00694-18. e00694-18.
[53] Belcher T, MacArthur I, King JD, Langridge GC, Mayho M, Parkhill J, et al. Fundamental differences in physiology of *Bordetella pertussis* dependent on the two-component system Bvg revealed by gene essentiality studies. Microb Genom 2020;6. https://doi.org/10.1099/mgen.0.000496.
[54] Gasperini G, Arato V, Pizza M, Aricò B, Leuzzi R. Physiopathological roles of spontaneously released outer membrane vesicles of *Bordetella pertussis*. Future Microbiol 2017;12:1247–59. https://doi.org/10.2217/fmb-2017-0064.
[55] Morse JH, Morse SI. Studies on the ultrastructure of *Bordetella pertussis*: I. Morphology, origin, and biological activity of structures present in the extracelluar fluid of liquid cultures of *Bordetella pertussis*. J Exp Med 1970;131:1342–57. https://doi.org/10.1084/jem.131.6.1342.
[56] Shrivastava R, Jiang X, Chng S-S. Outer membrane lipid homeostasis via retrograde phospholipid transport in *Escherichia coli*. Mol Microbiol 2017;106:395–408. https://doi.org/10.1111/mmi.13772.
[57] Nikaido H. Molecular basis of bacterial outer membrane permeability revisited. Microbiol Mol Biol Rev 2003;67:593–656. https://doi.org/10.1128/mmbr.67.4.593-656.2003.
[58] Nikaido H. Outer membrane of *Salmonella typhimurium* transmembrane diffusion of some hydrophobic substances. Biochim Biophys Acta 1976;433:118–32. https://doi.org/10.1016/0005-2736(76)90182-6.
[59] Parsons LM, Lin F, Orban J. Peptidoglycan recognition by Pal, an outer membrane lipoprotein. Biochemistry 2006;45:2122–8. https://doi.org/10.1021/bi052227i.
[60] Zückert WR. Secretion of bacterial lipoproteins: through the cytoplasmic membrane, the periplasm and beyond. Biochim Biophys Acta 2014;1843:1509–16. https://doi.org/10.1016/j.bbamcr.2014.04.022.
[61] Wang Y-H, Chen H-H, Huang Z, Li X-J, Zhou N, Liu C, et al. PapA, a peptidoglycan-associated protein, interacts with OmpC and maintains cell envelope integrity. Environ Microbiol 2021;23:600–12. https://doi.org/10.1111/1462-2920.15038.
[62] Volokhina EB, Beckers F, Tommassen J, Bos MP. The β-barrel outer membrane protein assembly complex of *Neisseria meningitidis*. J Bacteriol 2009;191:7074–85. https://doi.org/10.1128/JB.00737-09.
[63] McBroom AJ, Johnson AP, Vemulapalli S, Kuehn MJ. Outer membrane vesicle production by *Escherichia coli* is independent of membrane instability. J Bacteriol 2006;188:5385–92. https://doi.org/10.1128/JB.00498-06.
[64] Clavel T, Germon P, Vianney A, Portalier R, Lazzaroni JC. TolB protein of *Escherichia coli* K-12 interacts with the outer membrane peptidoglycan-associated proteins Pal, Lpp and OmpA. Mol Microbiol 1998;29:359–67. https://doi.org/10.1046/j.1365-2958.1998.00945.x.
[65] Cascales E, Lloubès R. Deletion analyses of the peptidoglycan-associated lipoprotein Pal reveals three independent binding sequences including a TolA box. Mol Microbiol 2004;51:873–85. https://doi.org/10.1046/j.1365-2958.2003.03881.x.
[66] Henderson B, Martin A. Bacterial virulence in the moonlight: multitasking bacterial moonlighting proteins are virulence determinants in infectious disease. Infect Immun 2011;79:3476–91. https://doi.org/10.1128/IAI.00179-11.
[67] Daleke-Schermerhorn MH, Felix T, Soprova Z, ten Hagen-Jongman CM, Vikström D, Majlessi L, et al. Decoration of outer membrane vesicles with multiple antigens by using an autotransporter approach. Appl Environ Microbiol 2014;80:5854–65. https://doi.org/10.1128/AEM.01941-14.
[68] Luu LDW, Octavia S, Aitken C, Zhong L, Raftery MJ, Sintchenko V, et al. Surfaceome analysis of Australian epidemic *Bordetella pertussis* reveals potential vaccine antigens. Vaccine 2020;38:539–48. https://doi.org/10.1016/j.vaccine.2019.10.062.
[69] Burns DL, Gould-Kostka JL, Kessel M, Arciniega JL. Purification and immunological characterization of a GroEL-like protein from *Bordetella pertussis*. Infect Immun 1991;59:1417–22. https://doi.org/10.1128/iai.59.4.1417-1422.1991.
[70] Yakhnina AA, Bernhardt TG. The Tol-Pal system is required for peptidoglycan-cleaving enzymes to complete bacterial cell division. Proc Natl Acad Sci U S A 2020;117:6777–83. https://doi.org/10.1073/pnas.1919267117.
[71] Meury J, Devilliers G. Impairment of cell division in *tolA* mutants of *Escherichia coli* at low and high medium osmolarities. Biol Cell 1999;91:67–75. https://doi.org/10.1111/j.1768-322x.1999.tb01085.x.
[72] Teleha MA, Miller AC, Larsen RA. Overexpression of the *Escherichia coli* TolQ protein leads to a null-FtsN-like division phenotype. Microbiologyopen 2013;2:618–32. https://doi.org/10.1002/mbo3.101.
[73] Frohlich BT, d'Alarcao M, Feldberg RS, Nicholson ML, Siber GR, Swartz RW. Formation and cell-medium partitioning of autoinhibitory free fatty acids and

cyclodextrin's effect in the cultivation of *Bordetella pertussis*. J Biotechnol 1996;45:137–48. https://doi.org/10.1016/0168-1656(95)00155-7.

[74] MacArthur I, Belcher T, King JD, Ramasamy V, Alhammadi M, Preston A. The evolution of *Bordetella pertussis* has selected for mutations of *acr* that lead to sensitivity to hydrophobic molecules and fatty acids. Emerg Microb Infect 2019;8:603–12. https://doi.org/10.1080/22221751.2019.1601502.

[75] Schoch TJ, Williams CB. Adsorption of fatty acid by the linear component of corn starch. J Am Chem Soc 1944;66:1232–3. https://doi.org/10.1021/ja01235a508.

[76] van Beek LF, de Gouw D, Eleveld MJ, Bootsma HJ, de Jonge MI, Mooi FR, et al. Adaptation of *Bordetella pertussis* to the respiratory tract. J Infect Dis 2018;217:1987–96. https://doi.org/10.1093/infdis/jiy125.

[77] Moon K, Bonocora RP, Kim DD, Chen Q, Wade JT, Stibitz S, et al. The BvgAS regulon of *Bordetella pertussis*. mBio 2017;8:e01526-17. https://doi.org/10.1128/mBio.

[78] Raeven RHM, van der Maas L, Tilstra W, Uittenbogaard JP, Bindels THE, Kuipers B, et al. Immunoproteomic profiling of *Bordetella pertussis* outer membrane vesicle vaccine reveals broad and balanced humoral immunogenicity. J Proteome Res 2015;14:2929–42. https://doi.org/10.1021/acs.jproteome.5b00258.

[79] Gasperini G, Biagini M, Arato V, Gianfaldoni C, Vadi A, Norais N, et al. Outer membrane vesicles (OMV)-based and proteomics-driven antigen selection identifies novel factors contributing to *Bordetella pertussis* adhesion to epithelial cells. Mol Cell Proteomics 2018;17:205–15. https://doi.org/10.1074/mcp.RA117.000045.